Genes & Diseases

SHORT COMMUNICATION

An eIF3a gene mutation dysregulates myocardium growth with left ventricular noncompaction via the p-ERK1/2 pathway

Mei Ge [a,b], Xuehan Bai [a,b], Aoyi Liu [a,b], Lingjuan Liu [a,b], Jie Tian [a,b], Tiewei Lu [a,b,*]

[a] Department of Cardiology, Children's Hospital of Chongqing Medical University, Chongqing, 401122, PR China
[b] China International Science and Technology Cooperation Center for Child Development and Critical Disorders, Chongqing Key Laboratory of Pediatrics, Ministry of Education Key Laboratory of Child Development and Disorders, Chongqing, 401122, PR China

Abstract Left ventricular noncompaction (LVNC) is a heterogeneous disorder with unclear genetic causes and an unknown mechanism. eIF3a, an important member of the Eukaryotic translation initiation factor 3 (eIF3) family, is involved in multiple biological processes, including cell proliferation and migration during myocardial development, suggesting it could play a role in LVNC development. To investigate the association between a novel variant (c.1145 A- > G) in eIF3a and LVNC, and explore potential mechanisms that could lead to the development of LVNC. A novel eIF3a variant, c.1145 A- > G, was identified by whole-exome sequencing in a familial pedigree with LVNC. Adenovirus vectors containing wild-type eIF3a and the mutated version were constructed and co-infected into H9C2 cells. Cell proliferation, apoptosis, cell migration, and differentiation, as well as phosphorylation of ERK1/2 were studied and were measured by proliferation assays, flow cytometry, real-time PCR and Western blot, respectively. The eIF3a mutation inhibited the proliferation of H9C2 cells, induced apoptosis, promoted cell migration, and inhibited the differentiation of human induced pluripotent stem cell-derived cardiomyocytes (hiPSC-CMs). The effect of the eIF3a mutation may be attributed to a decrease in expression of p-ERK1/2. A novel *eIF3a* gene mutation disrupted the p-ERK1/2 pathway and caused decreased myocardium proliferation, differentiation, accelerated migration.This finding may provide some insight into the mechanism involved in LVNC development.

* Corresponding author. Department of Cardiology, Children's Hospital of Chongqing Medical University, Chongqing, China.
   E-mail address: ltw@hospital.cqmu.edu.cn (T. Lu).

Introduction

Left ventricular non-compaction (LVNC), characterized by prominent and excessive trabeculations with deep recesses in the left ventricular wall,[1,2] ranks as the third most common form of cardiomyopathy.[3,4] Patients with LVNC can present different clinical phenotypes, and the prognosis is usually determined by the occurrence of complications including thromboembolism, arrhythmia and heart failure, even premature death.[1,5] LVNC is an inherited polygenic cardiomyopathy with a poorly understood etiology.[6] Therefore, it is necessary to explore the potential genetic causes of LVNC.

During mammalian heart development, the formation and compaction of trabecular have been identified as key steps in the formation of a complete and functional ventricular wall.[7,8] At the early stage of midgestation, myocardium and endocardium cell layers give rise to an early tubular heart. Directional migration of the monolayer of cardiomyocytes initiates formation of trabecular. Trabecular myocardium must proliferate in order to generate a sufficient number of myocytes to form a two-layer myocardium with compact and trabecular zones. At this point, these cells may either reduce their proliferative activity in order to undergo terminal differentiation and lineage specification.With cardiomyocytes further differentiate, proliferation and extending, it forms the protruding trabecular, which facilitate the exchange of oxygen and nutrients in the myocardiums.[9,10] At late midgestation, the myocardium undergoes compaction, through which a thicker, more compact ventricular wall forms.[11] Consequently, cardiac growth and chamber maturation both require a balance between proliferation and differentiation, and both processes must be controlled temporally, as well as spatially.

Eukaryotic translation initiation factor 3 (eIF3) has been shown to be a key factor of gene regulation at the transcriptional and translational levels.[12] eIF3a, the largest and most well-known member of the eIF family, is involved in regulating transcription, cell cycle timing, differentiation and migration.[13] Little has been reported, however, on the effect of eIF3a in the pathogenesis of cardiomyopathy. Our studies have detected a novel mutation in eIF3a, c.1145 A- > G, in a LVNC family, which we hypothesized was likely to be associated with the mechanism underlying LVNC development. Therefore, in this study, we sought to investigate the association between this novel mutation in eIF3a and LVNC, and to explore the potential mechanisms through which eIF3a could cause LVNC.

Materials and method

Subjects

A rare LVNC family pedigree was discovered at the Children's Hospital of Chongqing Medical University. Blood samples were collected from the propositus and her family (sister, mother and aunt) for DNA extraction and whole exome sequencing (WES) (Deyi Oriental Translational Medicine Research Center, China). The original WES data were analyzed to confirm the biological relationships between the daughters, their mother and their aunt. First, the mutations identified by WES were selected by bioinformatic analysis and then functional predictions were made using Genebank tools, including the UCSC Genome Browser (http://genome.ucsc.edu/), GENECARDS (https://www.genecards.org/), the NCBI database (https://www.ncbi.nlm.nih.gov/), UNIPROT (https://www.uniprot.org/), and STRING (https://string-db.org/). Then, well-conserved mutations that caused amino acid polarity changes in important functional domains were screened as possibly pathogenic for LVNC. The mutations were then confirmed by Sanger sequencing, using the Chromas software for data analysis.

Cell culture and transfections

H9C2 is a specific cardiac cell line with both skeletal and cardiac functions that is derived from embryonic rat ventricular tissue. Cells were cultured in Dulbecco's Modified Eagle Media (DMEM, Gibco) supplemented with 8% fetal bovine serum (FBS, Hyclone) and 100 mg/ml penicillin/streptomycin, and maintained at 37 °C with 5% CO_2. To prevent mycoplasma, 55 μl Plasmosin was added to 550 ml media. The adenovirus encoding mutated eIF3a, GFP and FLAG-tags was synthesized by Hanbio. The mutated Ad-eIF3a was transfected into the H9C2 cardiac muscle cell line to analyze the effect of the eIF3a mutation on the cells. Untransfected cells and Ad-GFP transfected cells were used as the blank control and AdGFP negative control, respectively. When the cells reached about 70−80% confluence, they were Co-transfected at an MOI of 300. After continuous transfection for 10 h, the media was removed and fresh medium was added.

The iPSC cells and iPSC-derived-cardiomyocytes had been successfully constructed in our previous work (Liu et al, the article has been accepted) and other team. The experimental protocol are definitive according to the paper.[14−16]

Quantitative real-time PCR

Total RNA was extracted using TRIzol Reagent (Sigma) 48 h after transfection. cDNA was synthesized using the Reverse Transcriptase kit (TaKaRa, NO:RR047A, China) and amplified with SYBR® Green Master Mix kit (Vazyme, China). Relative mRNA expression was determined using the 2-ΔΔCt method. Primers for the genes were synthesized by Life Technologies Corporation (Shanghai, China) and the sequences were as follows:

eIF3a: 5′-TTGCCACATTGCTAGGTC-3′ (forward primer).

5′-TCACTTCTGGGACAACAC-3′ (reverse primer).

Sox2: 5′-GCCGAGTGGAAACTTTTGTCG-3′ (forward primer).

5′-GCAGCGTGTACTTATCCTTCTT-3′ (reverse primer).

Oct4: 5′-CAGCGACTATGCACAACGAGA-3′ (forward primer).

5′-GCCCAGAGTGGTGACGGA-3′ (reverse primer).

Nkx2.5: 5′-TTCCCGCCGCCCCCGCCTTCTAT-3′ (forward primer).

5′-CGCTCCGCGTTGTCCGCCTCTGT-3′ (reverse primer).

cTnT: 5′-GGCAGCGGAAGAGGATGCTGAA-3′ (forward primer).

5′-GAGGCACCAAGTTGGGCATGAACGA-3′ (reverse primer).

β-actin: 5′-GGAGATTACTGCCCTGGCTCCTA-3′ (forward primer).

5′-GACTCATCGTACTCCTGCTTGCTG-3′ (reverse primer).

GAPDH: 5′-GAAATCCCATCACCATCTTCCAG-3′ (forward primer).

5′-AAATGAGCCCCAGCCTTCTC-3′ (reverse primer).

Cell proliferation assays

Cell proliferation was analyzed using the Cell Counting Kit-8 (CCK-8) assay (K1018, APExBIO). The H9C2 cells were plated in 96-well plates at a density of 1.5×10^3 cells/well. Following the manufacturer's protocol, cell proliferation was detected every 24 h. Briefly, 10 μl of CCK-8 solution was added to each well and incubated for 2 h at 37 °C. Then, the absorbance at 450 nm was measured for each solution using a spectrophotometer.

Cell cycle analysis

Approximately 1×10^6 H9C2 cells were fixed in 75% ethanol at 4 °C at least for 24 h. The fixed cells were then washed with PBS three times, and incubated with 100ul RNase A for 30 min at 37 °C. 400 μl of propidium iodide (PI) (KGA512, KeyGen, China) were then added to the cell suspension. The mixture was incubated for 30 min in the dark at room temperature. The suspended cells were analyzed using a FACS Calibur Flow Cytometer (BD Biosciences, San Jose, CA, USA).

Annexin V-APC/7-AAD assay for cellular apoptosis

Transfected H9C2 cells were seeded in 6 cm dishes at a density of 8×10^5 cells and incubated for 72 h. Then, to evaluate early and late apoptotic activity, an Annexin V-APC/7-AAD apoptosis detection kit was used according to the manufacturer's instructions. Cells were washed with cold PBS and then were resuspended in 500 μl of Binding Buffer. After cells were stained with 5 μl of Annexin V-APC and 5 μl of 7-AAD, they were immediately analyzed using a FACS Flow Cytometer (BD Biosciences, San Jose, CA, USA).

Cell migration assays

Transfected H9C2 cells were removed using 0.5 mM EDTA, counted and plated at 1×10^6 cells/mL in 6-well plates. Cells were incubated for 1 day, yielding confluent monolayers that could be used for wounding. Wounds were made using a 10 μl pipette tip, and images were taken at 0, 24 and 48 h after wounding. The distance migrated by the cell monolayer to close the wound area during this time period was measured using ImageJ. Experiments were carried out in triplicate and repeated a minimum of three times.

Immunofluorescence

When the cells were 30-40% confluent, they were washed three times with PBS, fixed in room temperature 4% paraformaldehyde for 20 min, and then washed again in PBS three times. Cells were permeabilized in 0.5% Triton X-100 in PBS for 5 min at room temperature and washed three times with PBS. After blocking with 5% BSA for 30 min at room temperature, the cells were incubated with anti-vinculin mouse polyclonal antibody (1:400 in PBS; V9131, Sigma) overnight at 4 °C. Cells were then washed in PBS and TRITC-conjugated goat-anti-mouse (1:200, T 5393, Sigma) was added and incubated in the dark at room temperature. Finally, the cells were washed again with PBS, stained with DAPI (Roche, 10236276001, 5 μg/ml) for 15 min at 37 °C, and then mounted in anti-fluorescent quencher (YEASEN, 36308ES11, Shanghai). These images were captured with NIH.

Western blot analysis of p-ERK1/2

Cells were washed with cold PBS and then were lysed in lysis buffer (KeyGEN BioTECH, NO: KGP250), supplemented with a protease and phosphatase inhibitors (Roche, Switzerland). The protein concentrations were measured using Coomassie (Bradford) Protein Assay (KeyGEN BioTECH, China). Sample proteins were separated on an SDS-PAGE gel and transferred into 0.22-μm PVDF membrane. After transferring, the membrane was blocked in 5% free-fat milk in TBST or 5% BSA for 1 h, and then incubated with primary antibodies overnight at 4 °C. Then, the membranes were washed with TBST three times, followed by incubation in secondary antibody. Finally, the protein bands were visualized using chemiluminescence and band intensity was analyzed and measured with ImageJ. The following antibodies were used: rabbit anti-p44/42 Erk1/2 (Cell signaling, 4695, USA, 1:1000), rabbit anti-phospho-p42/44 Erk1/2 (Cell signaling, 4370, USA, 1:2000), anti-vinculin (1:200; V9131, Sigma), anti-β-actin (4 A Biotech, China, 1:1000), goat anti-rabbit IgG (Millipore, GGHL-15 P, 1:10000) and goat anti-mouse IgG (Millipore, GGHL-90 P, 1:10000).

Statistics

All experiments were performed at least three times. Statistical analysis was performed in SPSS version 20. All data are expressed as mean ± SEM. Significance was determined using one-way analysis (ANOVA). $P < 0.05$ was considered statistically significant.

Result

## *eIF3a* gene mutation uncovered in patients of familial pedigree with LVNC

To investigate the potential genetic pathogenesis of LVNC, we recruited a family that had cases of LVNC. This study included the proband (III-1) and her elder sister, who were definitively diagnosed with LVNC based on clinical manifestations, echocardiography, and related examinations (Fig. 1A). Interestingly, their parents had normal clinical phenotypes. Fig. 1B shows the echocardiography analysis result of the proband, which indicated that the ratio of the thickness of the non-compact endocardial layer to the thickness of the compact epicardial layer was 2.076 (0.791/0.381). Genetic testing by whole-exome sequencing revealed a heterozygous variation, c.1145 A- > G present in exome 8 of eIF3a in the proband and her elder sister, but not in their mother or aunt (Fig. 1C). The mutation changes the amino acid from tyrosine (Tyr) to cysteine (Cys) at position 382 (Y382C) (Fig. 1D). This change occurs in the PCI domain that mediates protein—protein interactions and is at a site that is highly conserved among different species, suggesting it is an important functional region of the protein (Fig. 1E). The pedigree of the family studied suggests a correlation exists between the LVNC phenotype and the c. 1145 A- > G mutation.

Adenovirus vector validation and transfection

H9C2 cells were transfected with a vector expressing both GFP and a variant of eIF3a. After 48hrs, GFP expression was measured using fluorescence staining (Fig. 1F). Untransfected cells served as the control group and did not produce any fluorescence. Real-time PCR analysis showed that the relative levels of eIF3a mRNA in cells transfected with wild-type and mutant eIF3a were significantly higher than that of the untransfected and vector only controls at 48 h and 72 h post-transfection. No significant difference was found between the two control groups. These results indicated that transfection of a transgene encoding Eif3a carrying the c. 1145 A- > G mutation was successful and suitable for further study.
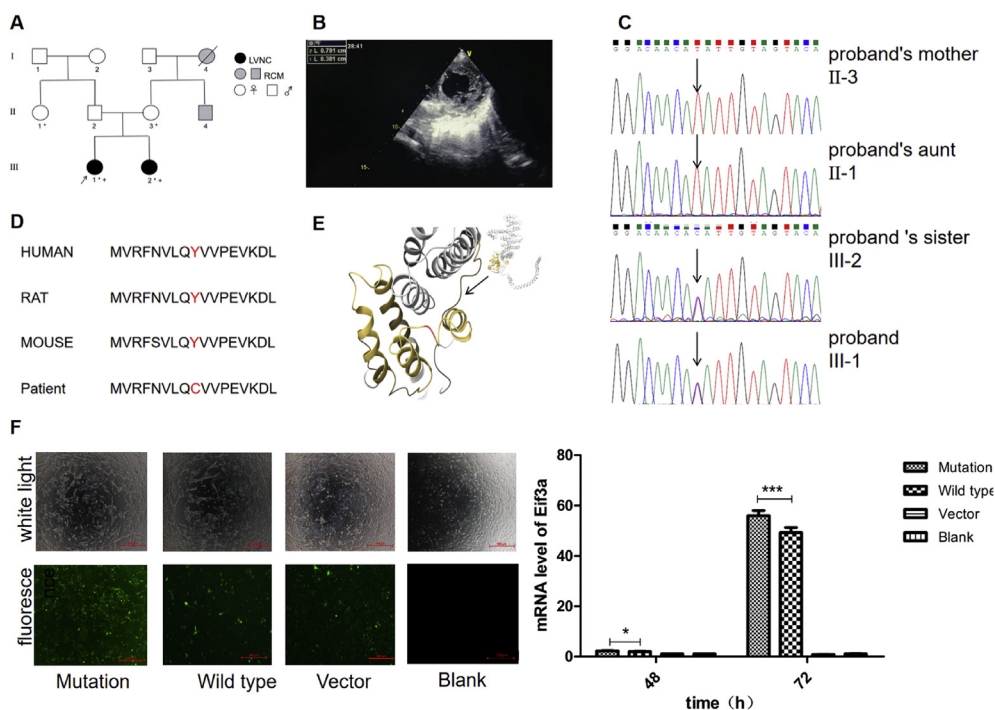
Figure 1 Characterization of LVNC patient carrying eIF3a (c.1145 A- > G) mutation and adenovirus vector transfection **(A)** A schematic of family LVNC pedigree, where the arrow indicates the proband (III-1). Mother (II-3), aunt (II-4) and sisters (III-1, III-2) underwent the whole exome sequencing and Sanger sequencing. Samples are marked with an asterisk. Plus and minus signs indicate the presence or absence of the eIF3a (c.1145 A- > G) mutation **(B)** The LVNC phenotype of the proband no. 1 (III-1) as assessed by echocardiography, which shows the thickness ratio of the non-compact endocardial layer compared to the compact epicardial layer was >2.0 (0.791/0.381). LA, left atrium; LV, left ventricle. Scale bars, 1 cm **(C)** Chromatograms depicting the sequencing results of the c.1145 A- > G variant in affected individuals and in a non-affected family member. Amino acids are also shown **(D)** Evolutionary conservation of *p.*382,Tyr(Y)-Cys(C) mutation in all species **(E)** Three-dimensional homology modeling of human eIF3a (*p.*382,Tyr(Y)-Cys(C), marked with red, PCI domain marked with yellow) mutated protein **(F)** transfected with Adenovirus encoding GFP in addition to c.1145 A- > G eIF3a, wild type eIF3a and blank vector, respectively, 48 h after transfection. Cell state and transfection efficiency of each group were observed using light and fluorescence microscopes. The level of eIF3a mRNA increased in the mutated and wild type groups 48 h post-transfection. Sanger sequencing was used to verify the mutation.*P < 0.05, ***P < 0.001. Error bars show mean ± standard deviation.

The Eif3a mutation inhibited proliferative capacity and induced apoptosis in H9C2 cells

To examine if the eIF3a mutation is associated with proliferation in H9C2 cells, CCK-8 assays were performed. We found that proliferation significantly decreased 72 h after transfection with the mutated eIF3a compared to the wild type (Fig. 2A) and this effect was maintained throughout the entire time-course. Interestingly, flow cytometry analysis of the DNA content of propidium iodide-stained H9C2 cells at G0/G1, S, and G2/M phases showed no statistically significant difference between the groups (Fig. 2B), meaning the decline proliferation does not come from impaired DNA synthesis. On the contrary, as shown in Fig. 2C, the number of apoptotic cells increased significantly in the group expressing mutated eIF3a compared to the group expressing the wild type version. These results indicated the eIF3a mutation reduced the proliferative capacity by inducing apoptosis in H9C2 cells.

The eIF3a mutation accelerated migration in H9C2 cells

Wound-healing assays were performed to assess the effect of mutant eIF3a on the cell migration abilities of H9C2 cells. H9C2 cells were scratched, and assessed for wound closure after 48 h. We found that the wound was mostly closed in the mutation and wild type group, and the closing rate in the mutated group was faster obviously. However, vector and blank group barely recovered from initial scratches

(Fig. 3A). These indicated that the eIF3a mutation accelerated cell migration abilities in H9C2 cells. To understand the cause of this accelerated cell migration, we analyzed the levels of vinculin, a protein which plays an important role in strengthening cell–extracellular matrix interactions,[17,18] using both immunofluorescence staining and western blot analysis. Expression of vinculin was higher in the mutation group compared to the wild type group (Fig. 3BC). These data show that mutated eIF3a increased the expression of vinculin, possibly causing increased migration of H9C2 cells.

eIF3a mutation inhibits cardiac differentiation in the development

To test whether the eIF3a mutation affects myocardial differentiation, we took advantage of human induced pluripotent stem cells (hiPSCs), a unique cellular model to study heart development. Cells were collected at different time points during hiPSC differentiation into cardiomyocytes. Stem cell gene markers declined gradually, while cardiac transcription factors increased during myocardial differentiation. In this study, at an early stage of hiPSC cardiomyocyte differentiation, the expression of the stem cell markers Oct-4 and Sox2 was higher in the mutation group than in the wild type group. At a later stage, however, when hiPSCs have already differentiated into mature myocardium, cTnT, a cardiomyocyte-specific marker, showed higher expression in the wild type group, compared with that of the mutation group. Additionally,
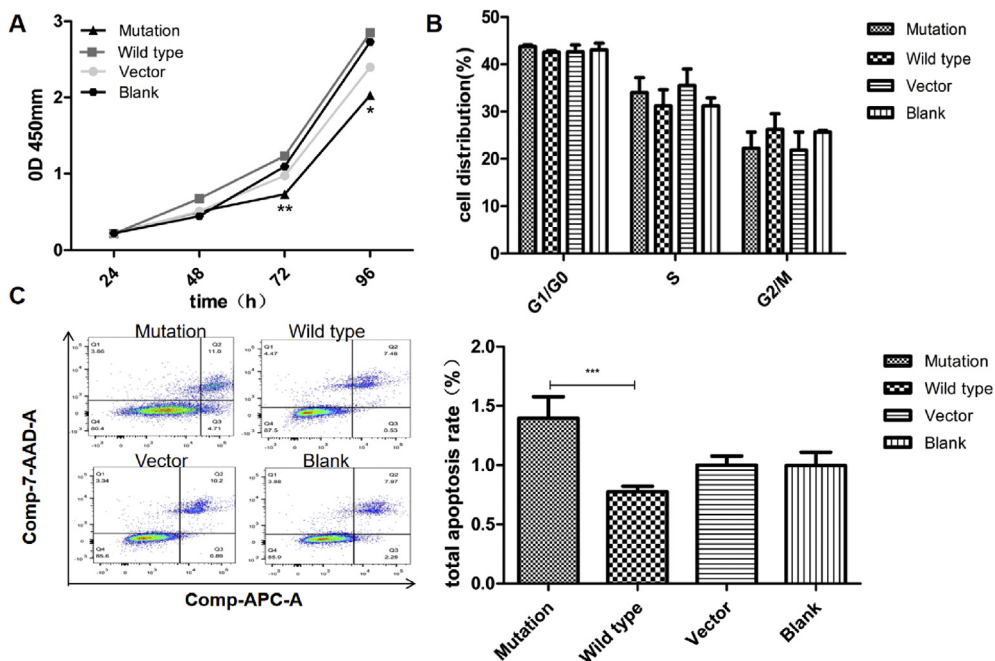
Figure 2   eIF3a mutation suppresses proliferation and induces apoptosis in H9c2 cells **(A)** CCK-8 assay results showing that H9C2 cell proliferation significantly decreased in the cells expressing mutated eIF3a compared to the wild type group **(B)** The DNA content of PI-stained H9C2 cells at the G0/G1, S, and G2/M phases as assessed by flow cytometry. There were no statistically significant differences between the groups **(C)** Apoptosis in H9C2 cells was measured by Annexin V-APC/7-AAD staining and flow cytometry and showed that the cells with mutated eIF3a had higher levels of apoptosis compared to the wild type group. *$P < 0.05$,**$P < 0.05$, ***$P < 0.001$. Error bars show mean $\pm$ standard deviation.
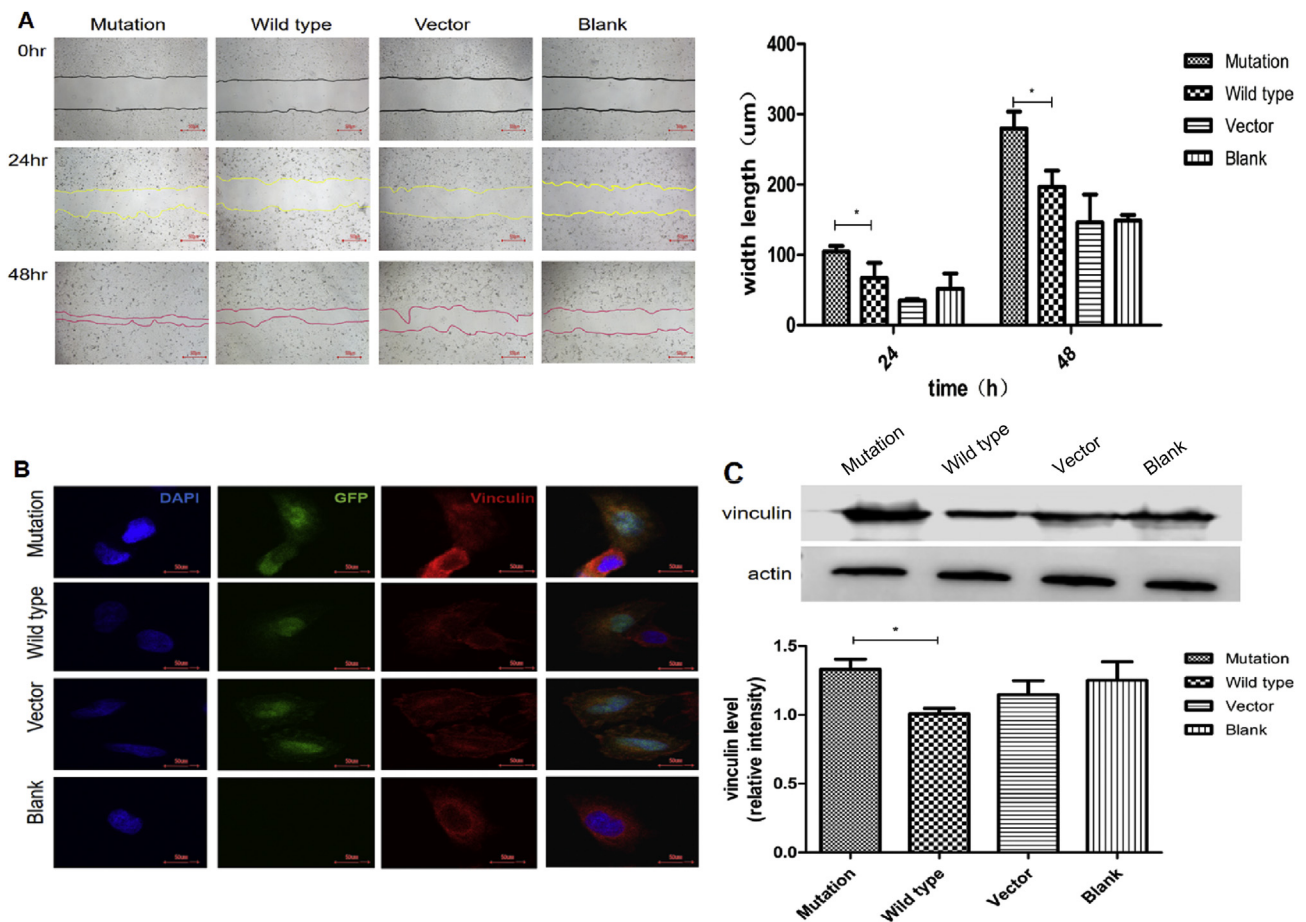
Figure 3   eIF3a mutation accelerates migration and motility in H9C2 cells **(A)** H9C2 cell migration as evaluated by wound healing showed that cells with mutated eIF3a migrate faster than others **(B)** Images showing vinculin protein in red and DAPI in blue. The expression of vinculin protein in cells expressing c.1145 A- > G eIF3a was higher compared to wild type cells **(C)** The expression of vinculin was determined by western blot. Quantification of vinculin intensity showed that the mutation group had higher expression than the wild type. *$P < 0.05$, Scale bar = 10 μm. Error bars show mean ± standard deviation.

expression of Nkx2.5, an early cardiomyocyte transcription factor, was higher in the mutation group than in the wild type group (Fig. 4). These results demonstrate that the eIF3a mutation might enhance the stemness of hiPSCs, while delaying cardiac differentiation during myocardial development.

Effect of eIF3a mutation on phosphorylation of ERK1/2

We sought to elucidate potential signaling pathways associated with the proliferation, migration and differentiation in myocardial development, as we figured the effects of the eIF3a mutation could be due to changes in these pathways. The activity of the ERK1/2 signaling pathway, an important pathway involved in multiple processes including cellular proliferation and differentiation, was detected by western blot. We found that the expression of phosphorylated ERK1/2 decreased in the mutation group compared to the wild type group (Fig. 5A). In addition, there was a clear

reduction in the translocation of pERK1/2 to the nucleus in the presence of mutated eIF3a (Fig. 5B). These results suggest that the eIF3a c.1145 A- > G mutation may reduce the proliferation, migration and differentiation ability of cardiomyocytes by inhibiting the p-ERK1/2 pathway.

Discussion

LVNC is a polygenic heterogenic cardiomyopathy.[19] Some genes, mainly encoding proteins involved in the cytoskeleton, sarcomere, mitochondria and ion channels, have been reported to be associated with clinical LVNC phenotypes.[20,21] In the past decade, many efforts have been made to build a LVNC mouse model and to study the disease mechanisms in humans. Some of these studies are described below. Mutations in SRC-1/3, proteins necessary for myocardial cell proliferation and differentiation, caused the formation of prominent myocardial trabecular, deep intertrabecular recesses and thin ventricular walls in mice, similar to the noncompaction ventricular phenotypes
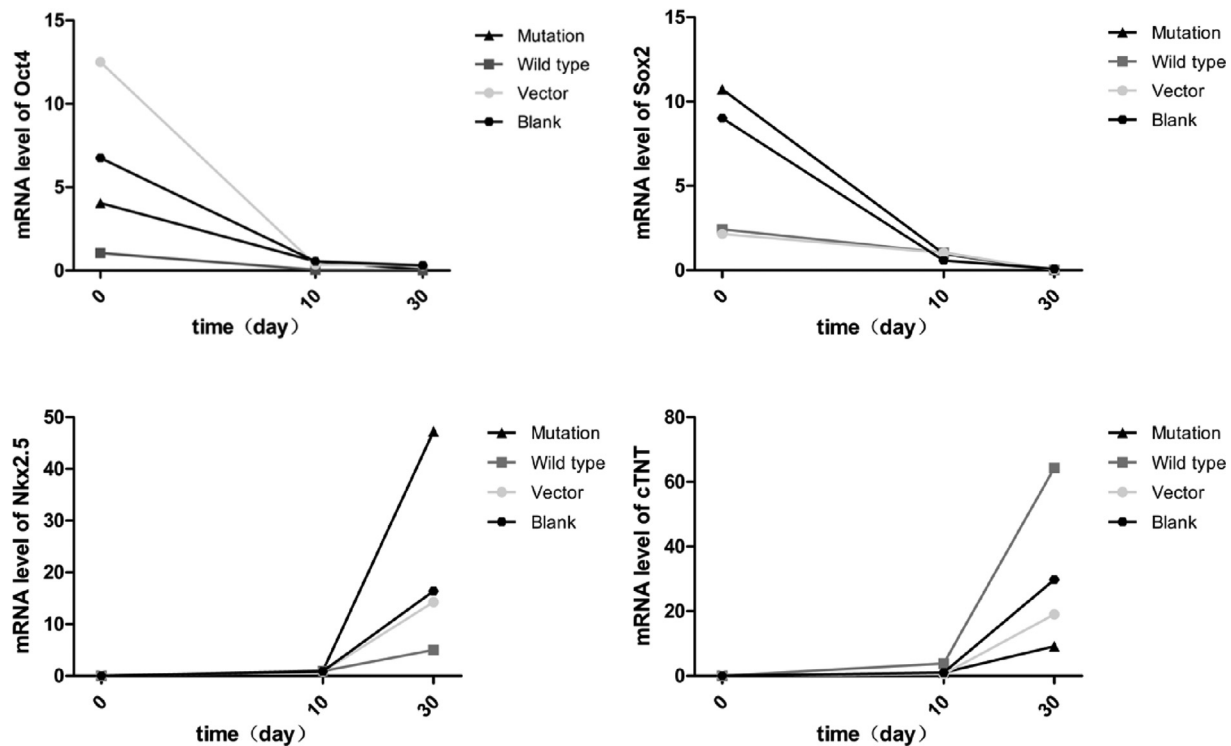
Figure 4 eIF3a mutation inhibits cardiac differentiation during development. The mRNA level of Sox2, Oct4, Nkx2.5, cTnT in cardiac development were determined by RT-qPCR. Mutation of eIF3a led to strong expression of stem cell gene makers early in development and delayed expression of myocardial differentiation regulators.

seen in humans.[22] Decreased cell proliferation in the compacting layer was observed in early embryonic ($E < 13.5$) TAZ-KD mice.[23] Similar defects were also observed in Fkbp1a, Jarid2 and mib1-deficient mice.[24-26] Kodo et al used patient-specific induced pluripotent stem cell-derived cardiomyocytes study LVNC pathogenesis at the single-cell level, and found that LVNC iPSC-CMs had a reduced proliferation ability.[27] Shou et al[11] compiled a critical review of previous research of LVNC disease models, and concluded that in the different models, ventricular trabeculation and compaction is affected by regulating cell proliferation, cell polarization and myofibrillogenesis. Thus, protrusion of trabecular and complete formation of the ventricular conduction system can attributed to proliferation and differentiation of cardiomyocytes at the early stages of heart development, and these processes play an important role in the pathogenesis of LVNC. Therefore, the regulatory patterns and underlying mechanisms of these processes largely determine the pathogenesis of LVNC.

In this study, a c.1145 A- > G mutation in the *eIF3a* gene was detected in familial pedigree of LVNC and identified as potentially pathogenic gene. Previous studies reported that eIF3a was highly expressed in various tumor tissues and considered to be a tumor promoting factor because of its potential role in malignant transformation and cell growth.[28,29] miR-488-regulated inhibition of eIF3a was found to reduce the proliferation and migration ability in non-small-cell lung cancer (NSCLC).[30] However, there has been little work done to elucidate the relationship between

eIF3a and LVNC. We used H9C2 cells to simulate the embryonic myocardium of the mammalian heart and the novel c. 1145 A- > G eIF3a mutation identified in this study to observe the mechanisms underlying proper heart development and elucidate a possible connection between the mutation and the development of LVNC. Our results show that this eIF3a mutation could promote migration and reduce the proliferation by promoting apoptosis. Additionally, the effect of this mutation on the expression of stem cell and cardiomyocyte markers during cardiac differentiation was analyzed. It was previously determined that the differentiation of hiPSCs into cardiomyocytes is a good simulator for myocardial development. As expression of stem cell gene markers such as Oct-4 and Sox2 decline gradually while the expression of cardiomyocyte markers such as Nkx2.5 and cTnT increased,[31] Nkx2.5 is an early cardiac transcriptional regulator that is critical for mesoderm development into cardiac muscle cells and mutation of Nkx2.5 can lead to cardiac developmental defects such as ASD, VSD and atrioventricular block,[32-34] while cTnT is closely related to cardiac contraction,[35] which marks the maturation of myocardium. Our results show that mutation of eIF3a prevents the decrease of Oct-4 and Sox2, and delays the expression of Nkx2.5 and cTnT. Thus, the eIF3a mutation preserved cells in a naive state and inhibited myocardial differentiation, which may explain why the novel c.1145 A- > G mutation is associated with an increased risk of LVNC.

Previous studies have attempted to elucidate the signaling pathways involved in LVNC. In one study, protein
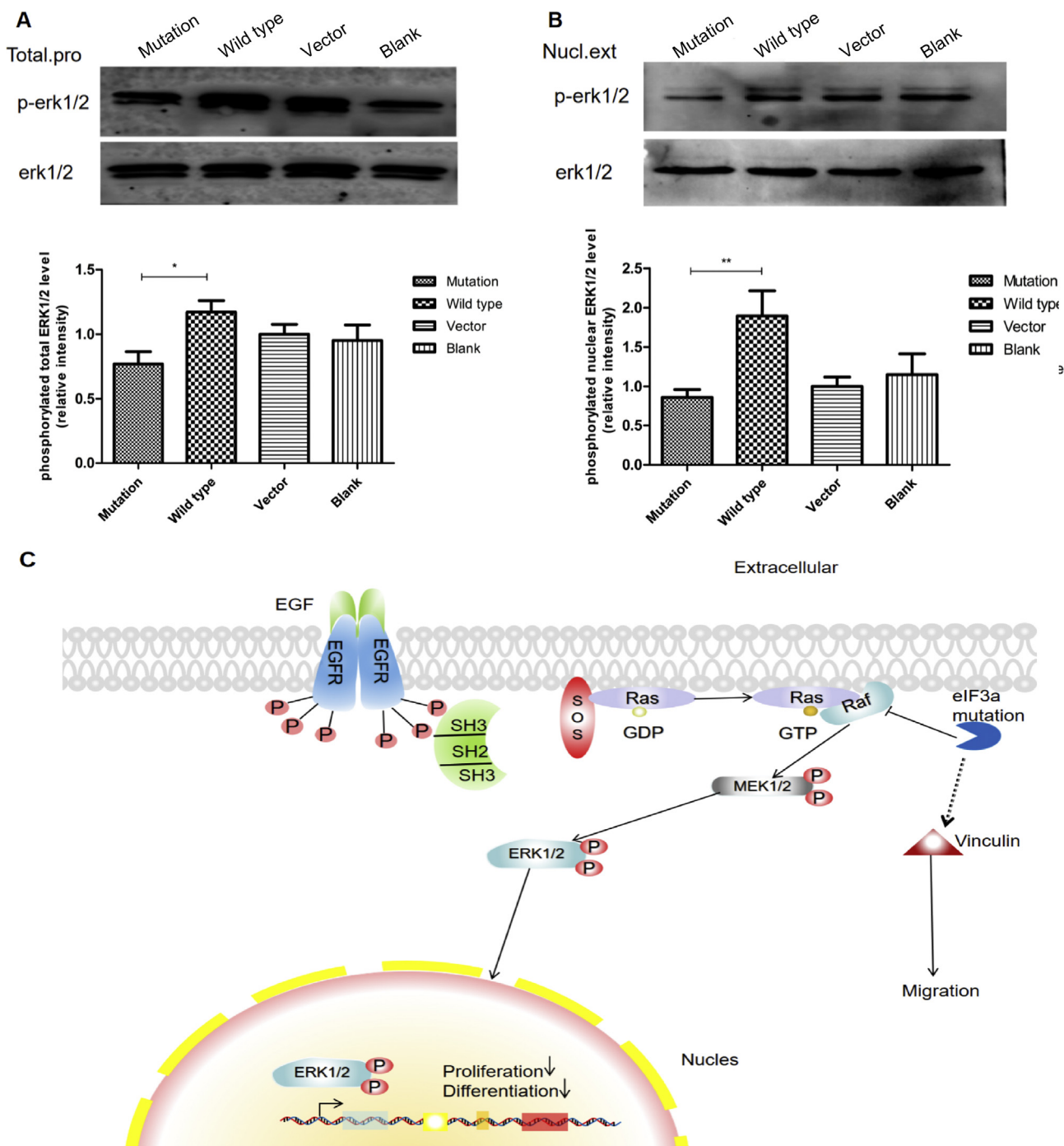
Figure 5 eIF3a mutation decreases phosphorylation of erk1/2. **(A)** The activity of ERK1/2 signal pathway as detected by western blot. Total ERK1/2 was used as a loading control. The expression level of phosphorylated ERK1/2 decreased in mutated eIF3a cells compared to wild type cells. Quantification of western blot measurements of p-ERK1/2 using total ERK1/2 as a control is shown **(B)** Nuclear translocation of pERK1/2 in cells expressing mutated eIF3a was higher than the wild type group. Quantification of western blot measurements was performed as described above. *$P < 0.05$, **$P < 0.05$. Error bars show mean $\pm$ standard deviation **(C)** Proposed mechanism of eIF3a mutation function in cardiomyocyte.

profiling of LVNC patients showed the highest correlation with dysregulated MAPK1 pathway,[36] similar to what was found in genetically modified mice models.[37] Other studies showed that Rxra-deficient mice had reduced ERK1/2 activity, leading to a thin-walled noncompaction ventricle and decreased levels of proliferation.[38] Previous studies have connected the classical RAS-RAF-MEK1/2-ERK1/2 signaling cascade to cell growth, proliferation, migration and differentiation. Nuclear translocation of Erk contributes to the proliferation and differentiation of myocytes specifically.[39] eIF3a binds to SHC and Raf-1, two components of the ERK1/2 pathway, to negatively regulate this

pathway.[40,41] Regulation of Raf-1 by RUVBL1 has been shown to affect the RAF/MEK/ERK pathway in lung adenocarcinoma tissues. Similar to regulation of this pathway by RUVBL1[42], we hypothesized regulation of the ERK1/2 pathway by eIF3a might be a potential mechanism for myocardial densification. Our results verified that eIF3a mutation can downregulate the phosphorylation of ERK1/2, particularly in the nucleus, which can also cause the changes we observed in proliferation and differentiation, and it also accelerate migration by down-regulate vinculin (Fig. 5C).

We have found that the novel c.1145 A- > G mutation in eIF3a can increase the risk of developing LVNC by dysregulation of the p-ERK1/2 pathway. Our conclusions were drawn from cell culture experiments, however, and it has been shown that using animal models or living human tissues is the most effective way to study clinical diseases.[11] Unfortunately, there is no well-established animal model for LVNC. Furthermore, it is difficult to obtain clinical tissue samples. In our lab, we used normal patient urinary cells and generated induced pluripotent stem cell-derived cardiomyocytes (iPSC-CMs), which not only avoid the ethical issues surrounding human tissue use but also carry a genetic background similar to the disease, making iPSC-CMs a powerful tool for studying the genetic mechanism of diseases. In the future, we will attempt to suppress eIF3a by gene silencing technology in iPSC-CMs derived from LVNC patients in order to further understand its mechanism.

In conclusion, the data we presented here demonstrate that the novel c.1145 A- > G eIF3a mutation inhibited proliferation and differentiation, accelerated migration via the p-ERK1/2 pathway, which may be involved in the pathogenesis of LVNC. Thus, our results may provide clues to help understand the underlying causes of LVNC, as well as information that could inspire new ideas for the prevention and treatment of LVNC.

Conclusion

Our findings indicate that the missense variant of the *eIF3a* gene, c.1145 A- > G, might be related to the development of LVNC. This mutation could possibly lead to dysregulation of myocardium proliferation, migration and differentiation via the p-ERK1/2 pathway. This alters cardiac development and could increase the risk of LVNC. These findings may provide a better understanding of the genetic basis of cardiac cell proliferation and differentiation, as well as the pathogenesis of LVNC, potentially leading to new approaches to both treat LVNC and reduce its prevalence through early gene intervention.

Conflict of Interests

The authors declare no conflict of interest.

Funding

Acknowledgements

Appendix A. Supplementary data

Supplementary data related to this article can be found at https://doi.org/10.1016/j.gendis.2020.02.003.

References

1. Arbustini E, Favalli V, Narula N, Serio A, Grasso M. Left ventricular noncompaction: a distinct genetic cardiomyopathy. *J Am Coll Cardiol*. 2016;68(9):949–966.
2. Sedmera D, Pexieder T, Vuillemin M, Thompson RP, Anderson RH. Developmental patterning of the myocardium. *Anat Rec*. 2000;258(4):319–337.
3. Nugent AW, Daubeney PE, Chondros P, et al. The epidemiology of childhood cardiomyopathy in Australia. *N Engl J Med*. 2003; 348(17):1639–1646.
4. Nugent AW, Daubeney PE, Chondros P, et al. Clinical features and outcomes of childhood hypertrophic cardiomyopathy: results from a national population-based study. *Circulation*. 2005;112(9):1332–1338.
5. Towbin JA. *Left Ventricular Noncompaction Cardiomyopathy*. In: *Heart Failure in the Child and Young Adult*. 2018.
6. Finsterer J. Inherited mitochondrial neuropathies. *J Neurol Sci*. 2011;304(1–2):9–16.
7. Jensen B, van der Wal AC, Afm M, Christoffels VM. Excessive trabeculations in noncompaction do not have the embryonic identity. *Int J Cardiol*. 2017;227:325–330.
8. Choquet C, Kelly RG, Miquerol L. Defects in trabecular development contribute to left ventricular noncompaction. *Pediatr Cardiol*. 2019;40(7):1331–1338.
9. Günthel M, Barnett P, Christoffels VM. Development, proliferation, and growth of the mammalian heart. *Mol Ther*. 2018; 26(7):1599–1609.
10. Wu M. Mechanisms of trabecular formation and specification during cardiogenesis. *Pediatr Cardiol*. 2018;39(6):1082–1089.
11. Liu Y, Chen H, Shou W. Potential common pathogenic pathways for the left ventricular noncompaction cardiomyopathy (LVNC). *Pediatr Cardiol*. 2018;39(6):1099–1106.
12. Saletta F, Suryo RY, Richardson DR. The translational regulator eIF3a: the tricky eIF3 subunit. *Biochim Biophys Acta*. 2010; 1806(2):275–286.
13. Li WQ, Li XH, Wu YH, et al. Role of eukaryotic translation initiation factors 3a in hypoxia-induced right ventricular remodeling of rats. *Life Sci*. 2016;144:61–68.
14. Jiang Q, Li K, Lu W, et al. Identification of small-molecule ion channel modulators in C. elegans channelopathy models. *Nat Commun*. 2018;9(1), e3941.
15. Yu Y, Sun S, Wang S, et al. Liensinine-and neferine-induced cardiotoxicity in primary neonatal rat cardiomyocytes and human-induced pluripotent stem cell-derived cardiomyocytes. *Int J Mol Sci*. 2016;17(2), e186.
16. Ke B, Zeng Y, Zhao Z, et al. Uric acid: a potent molecular contributor to pluripotent stem cell cardiac differentiation via mesoderm specification. *Cell Death Differ*. 2019;26(5): 826–842.
17. Polio SR, Stasiak SE, Jamieson RR, Balestrini JL, Krishnan R, Parameswaran H. Extracellular matrix stiffness regulates

human airway smooth muscle contraction by altering the cell-cell coupling. *Sci Rep*. 2019;9(1), e9564.

18. Bays JL, DeMali KA. Vinculin in cell—cell and cell—matrix adhesions. *Cell Mol Life Sci*. 2017;74(16):2999—3009.

19. Wijeyeratne YD, Behr ER. Recent developments in the genetics of cardiomyopathies. *Curr Genet Med Rep*. 2013;1(1):21—29.

20. Towbin JA, Jefferies JL. Response by towbin and jefferies to letter regarding article, "cardiomyopathies due to left ventricular noncompaction, mitochondrial and storage diseases, and inborn errors of metabolism. *Circ Res*. 2017;121(12), e90.

21. Towbin JA. Left ventricular noncompaction: a new form of heart failure. *Heart Fail Clin*. 2010;6(4):453—469.

22. Chen X, Qin L, Liu Z, Liao L, Martin JF, Xu J. Knockout of SRC-1 and SRC-3 in mice decreases cardiomyocyte proliferation and causes a noncompaction cardiomyopathy phenotype. *Int J Biol Sci*. 2015;11(9):1056—1072.

23. Phoon CK, Acehan D, Schlame M, et al. Tafazzin knockdown in mice leads to a developmental cardiomyopathy with early diastolic dysfunction preceding myocardial noncompaction. *J Am Heart Assoc*. 2012;1(2): jah3-e000455.

24. Luxán G, Casanova JC, Martínez-Poveda B, et al. Mutations in the NOTCH pathway regulator MIB1 cause left ventricular noncompaction cardiomyopathy. *Nat Med*. 2013;19(2): 193—201.

25. Cho E, Mysliwiec MR, Carlson CD, Ansari A, Schwartz RJ, Lee Y. Cardiac-specific developmental and epigenetic functions of Jarid2 during embryonic development. *J Biol Chem*. 2018; 293(30):11659—11673.

26. Shou W, Aghdasi B, Armstrong DL, et al. Cardiac defects and altered ryanodine receptor function in mice lacking FKBP12. *Nature*. 1998;391(6666):489—492.

27. Kodo K, Ong SG, Jahanbani F, et al. iPSC-derived cardiomyocytes reveal abnormal TGF-β signalling in left ventricular non-compaction cardiomyopathy. *Nat Cell Biol*. 2016; 18(10):1031—1042.

28. Pincheira R, Chen Q, Zhang JT. Identification of a 170-kDa protein over-expressed in lung cancers. *Br J Canc*. 2001; 84(11):1520—1527.

29. Chen G, Burger MM. p150 overexpression in gastric carcinoma: the association with p53, apoptosis and cell proliferation. *Int J Canc*. 2004;112(3):393—398.

30. Fang C, Chen YX, Wu NY, et al. MiR-488 inhibits proliferation and cisplatin sensibility in non-small-cell lung cancer (NSCLC) cells by activating the eIF3a-mediated NER signaling pathway. *Sci Rep*. 2017;7, e40384.

31. Kadota S, Pabon L, Reinecke H, Murry CE. In vivo maturation of human induced pluripotent stem cell-derived cardiomyocytes in neonatal and adult rat hearts. *Stem Cell Reports*. 2017;8(2): 278—289.

32. Tu CT, Yang TC, Tsai HJ. Nkx2.7 and Nkx2.5 function redundantly and are required for cardiac morphogenesis of zebrafish embryos. *PloS One*. 2009;4(1), e4249.

33. Ashraf H, Pradhan L, Chang EI, et al. A mouse model of human congenital heart disease: high incidence of diverse cardiac anomalies and ventricular noncompaction produced by heterozygous Nkx2-5 homeodomain missense mutation. *Circ Cardiovasc Genet*. 2014;7(4):423—433.

34. Serpooshan V, Liu Y, Buikema JW, et al. Nkx2.5+ Cardiomyoblasts contribute to cardiomyogenesis in the neonatal heart. *Sci Rep*. 2017;7(1), 12590.

35. Gomes AV, Potter JD, Szczesna-Cordary D. The role of troponins in muscle contraction. *IUBMB Life*. 2002;54(6):323—333.

36. Du H, Liu S, Li C, Wei Y. Comparative proteomics analysis of myocardium in left ventricular non-compaction cardiomyopathy. *Acta Biochim Biophys Sin*. 2019;51(6):653—655.

37. Nakamura T, Colbert M, Krenz M, et al. Mediating ERK 1/2 signaling rescues congenital heart defects in a mouse model of Noonan syndrome. *J Clin Invest*. 2007;117(8):2123—2132.

38. Sucov HM, Dyson E, Gumeringer CL, Price J, Chien KR, Evans RM. RXR alpha mutant mice establish a genetic basis for vitamin A signaling in heart morphogenesis. *Genes Dev*. 1994; 8(9):1007—1018.

39. Schevzov G, Kee AJ, Wang B, et al. Regulation of cell proliferation by ERK and signal-dependent nuclear translocation of ERK is dependent on Tm5NM1-containing actin filaments. *Mol Biol Cell*. 2015;26(13):2475—2490.

40. Xu TR, Lu RF, Romano D, et al. Eukaryotic translation initiation factor 3, subunit a, regulates the extracellular signal-regulated kinase pathway. *Mol Cell Biol*. 2012;32(1):88—95.

41. An S, Yang Y, Ward R, Liu Y, Guo XX, Xu TR. Raf-interactome in tuning the complexity and diversity of Raf function. *FEBS J*. 2015;282(1):32—53.

42. Guo H, Zhang XY, Peng J, et al. RUVBL1, a novel C-RAF-binding protein, activates the RAF/MEK/ERK pathway to promote lung cancer tumorigenesis. *Biochem Biophys Res Commun*. 2018; 498(4):932—939.